



OPEN

DATA DESCRIPTOR

A chromosome-level genome assembly of the gall maker pest inquiline, *Diomorus aiolomorphi* Kamijo (Hymenoptera: Torymidae)

Ruizhong Yuan^{1,2,3,6}, Qiuyu Qu^{1,2,3,4,6}, Zhaohe Lu^{1,2,3}, Xiansheng Geng⁵, Shiji Tian^{1,2}, Yu Jin^{1,2}, Jiabao Gong^{1,2,3}, Xiqian Ye^{1,2,3}, Pu Tang^{1,2,3}✉ & Xuexin Chen^{1,2,3,4}✉

Diomorus aiolomorphi Kamijo (Hymenoptera: Torymidae) is an inquiline of gall maker *Aiolomorpha rhopaloides* Walker (Hymenoptera: Eurytomidae). They are of significant economic significance and predominantly inhabit bamboo forest. So far, only four scaffold-level genomes have been published for the family Torymidae. In this study, we present a high-quality genome assembly of *D. aiolomorphi* at the chromosome level, achieved through the integration of Nanopore (ONT) long-read, Illumina pair-end DNA short-read, and High-through Chromosome Conformation Capture (Hi-C) sequencing methods. The final assembly was 1,084.56 Mb in genome size, with 1,083.41 Mb (99.89%) assigned to five pseudochromosomes. The scaffold N50 length reached 224.87 Mb, and the complete Benchmarking Universal Single-Copy Orthologs (BUSCO) score was 97.3%. The genome contained 762.12 Mb of repetitive elements, accounting for 70.27% of the total genome size. A total of 18,011 protein-coding genes were predicted, with 17,829 genes being functionally annotated. The high-quality genome assembly of *D. aiolomorphi* presented in this study will serve as a valuable genomic resource for future research on parasitoid wasps. The results of this study may also contribute to the development of biological control strategies for pest management in bamboo forests, enhancing ecological balance and economic sustainability.

Background & Summary

Diomorus aiolomorphi Kamijo (Hymenoptera: Torymidae) is a parasitic inquiline associated with the gall maker *Aiolomorpha rhopaloides* Walker (Hymenoptera: Eurytomidae). *D. aiolomorphi* and *A. rhopaloides* are of significant economic significance and predominantly inhabit bamboo forest. Notably, these two species constitute approximately 90% of the insects within this group in such environments¹.

The gall maker *A. rhopaloides* lays its eggs in the internode at the base of the new branch buds, stimulating the parapsylem tissue in these areas. This process inhibits the growth of bamboo plants, leading to a reduction in both the quantity and quality of bamboo shoots. It has been observed that bamboo galls are contagiously distributed across both the culms and branches in a bamboo stand^{2,3}. Its harm makes it a significant factor hindering effective management and economic value of bamboo forests, with notable impacts on both society and the environment⁴. It not only leads to reduced bamboo yield, lower quality, and decreased market prices but also results in indirect losses such as control and restoration costs and ecological impacts²⁻⁵. Adults of *D. aiolomorphi*, known as inquilines, oviposit on these young bamboo galls. Unlike typical phytophagous insects, *D. aiolomorphi* cannot create its own galls but instead feeds on the gall tissues induced by other gall makers^{4,5}. Understanding the attack pattern of *D. aiolomorphi* on bamboo galls is crucial for assessing and managing the

¹Institute of Insect Sciences, College of Agriculture and Biotechnology, Zhejiang University, Hangzhou, 310058, China. ²State Key Lab of Rice Biology, Ministry of Agriculture and Rural Affairs Key Lab of Molecular Biology of Crop Pathogens and Insects, and Zhejiang Provincial Key Laboratory of Biology of Crop Pathogens and Insects, Zhejiang University, Hangzhou, 310058, China. ³Guangdong Laboratory for Lingnan Modern Agriculture, Guangzhou, 510642, China. ⁴Hainan Institute, Zhejiang University, Sanya, 572025, China. ⁵Research Institute of Subtropical Forestry, Chinese Academy of Forestry, Hangzhou, 311400, China. ⁶These authors contributed equally: Ruizhong Yuan, Qiuyu Qu. ✉e-mail: ptang@zju.edu.cn; xxchen@zju.edu.cn

Sequencing strategy	Platform	Usage	Insertion size	Raw data (Gb)	Coverage (X)
Short-reads	Illumina	Genome survey	350 bp	28.37	26.16
Long-reads	Nanopore	Assembly	12–20 kb	81.21	74.88
Hi-C	Illumina	Hi-C assembly	350 bp	110.44	101.82
RNA-seq	Illumina	Annotation	350 bp	4.73	4.36

Table 1. Library sequencing data and methods used to assemble the *D. aiolomorphi* genome.

population density of *A. rhopaloides*¹. Despite the commonality of *D. aiolomorphi* among gall makers and its economic significance, it has received relatively little scientific attention⁶. Consequently, there is a substantial gap in our understanding of the genetic makeup underpinning the genome of *D. aiolomorphi*.

In this study, we have assembled the chromosome-level genome of *D. aiolomorphi*, representing the first chromosome-level sequenced genome of the family Torymidae. The genome size is 1,084.56 Mb, with 1,083.41 Mb (99.89%) assigned to five pseudochromosomes. The scaffold N50 of the genome is 224.87 Mb in length, and the complete Benchmarking Universal Single-Copy Orthologs (BUSCO) score reached 97.3%. A total of 762.12 Mb repetitive elements were identified, accounting for 70.27% of the total genome size. 18,011 protein-coding genes, with functional annotations available for 17,829 of these genes. The high-quality genome assembly of *D. aiolomorphi* provides a valuable repository for understanding the genomic traits of the Torymidae genomes.

Methods

Sampling. Galls were sampled from bamboo branches at Fuyang, Hangzhou, China (30°03' N, 119°57' E) before gall maker emergence, and a total of 1,467 galls were collected. An inquiline is an organism that lives within or on the structure of another organism. The inquiline, *D. aiolomorphi*, emerged from galls 15–20 days later than the gall maker *A. rhopaloides*. Before sequencing, both morphological examination⁷ and COI barcode information confirmed the identification of the species as *D. aiolomorphi*. The specimens were deposited at the Institute of Insect Sciences, Zhejiang University (ZJUH_20231101). They were preserved in 100% ethanol prior to DNA extraction to maintain the integrity of the genetic material, and subsequently kept in the scientific specimen repository.

Library preparation and genomic DNA sequencing. Genomic DNA was prepared by the sodium dodecyl sulfate (SDS) method followed by purification with QIAGEN[®] Genomic kit (Qiagen, Hilden, Germany) according to the manufacturer's standard operating procedure for both long-read and short-read whole genome sequencing (<https://www.qiagen.com/us/resources/resourcedetail?id=566f1cb1-4ffe-4225-a6de-6bd3261dc920&lang=en>). RNA extraction was conducted with the TRIzol reagent (Vazyme, Nanjing, China) (<https://bio.vazyme.com/product/730.html>). The quality of the extracted RNA was assessed using an Agilent 2100 Bioanalyzer (Agilent Technologies, Santa Clara, CA, USA). The RNA Integrity Number (RIN) was determined for each sample, ensuring that only high-quality RNA (RIN > 7.0) was used for subsequent sequencing processes. The total data produced from RNA extraction amounted to 4.73 Gb, with a duplication rate of 66.07%. The Q20 (Quality scores > 20) bases totaled 3,607,313,837 (97.8713%), while the Q30 (Quality scores > 30) bases amounted to 3,455,480,380 (93.7518%). Long-read sequencing was performed on the Nanopore GridION X5/PromethION sequencer (Oxford Nanopore Technologies, UK) at Nextomics. Short-read and transcriptome sequencing were sequenced on the Illumina Novaseq/MGI-2000 platforms. The total data generated from the long-read sequencing was 81.21 Gb, while the output from the short-read sequencing totaled 28.37 Gb (Table 1).

Genome survey and assembly. K-mer analysis was performed using Illumina paired-end sequenced DNA reads. This analysis was conducted before genome assembly to estimate the genome size and the level of heterozygosity. Briefly, quality-filtered reads were subjected to a 21-mer frequency distribution analysis employing Jellyfish v2.2.10⁸. For a read of length L, the number of k-mer produced is (L - 21 + 1). Therefore, the genome size (G) is estimated by the formula: $G = K_{\text{number}} / K_{\text{depth}}$, where K_{number} represents the total number of k-mer produced and K_{depth} represents the peak value of k-mer depth. Furthermore, the overall genomic properties were inferred by GenomeScope v1.0⁹. The preliminary genome survey of *D. aiolomorphi* revealed a low level of heterozygosity level (0.19%) within a substantial genome, 988,63 Mb. This estimated genome size was used to evaluate the integrity of the subsequent assembly (Fig. 1, Supplementary Table S1).

The primary assembly of the clean reads obtained from the Nanopore platform was conducted using nextDenovo v2.5.0¹⁰, and subsequently corrected using Canu v2.1.1¹¹. Illumina paired-end sequenced DNA reads were then utilized to polish and enhance the genome assembly using nextPolish v1.4.0¹². To eliminate haplotigs and contig overlaps in the *de novo* assembly, purge_dups v1.2.5 (https://github.com/dfguan/purge_dups) was employed. Finally, the primary assembly yielded 147 scaffolds with 1,084.58 Mb in genome size, 18.13 Mb in contig N50 and 224.87 Mb in scaffold N50.

Chromosome Hi-C assembly. The High-through Chromosome Conformation Capture (Hi-C) method¹³ was utilized to anchor accurately position hybrid scaffolds onto chromosomes. Genomic DNA was extracted from the thorax of an individual *D. aiolomorphi* for the Hi-C library. This library, along with the sequencing data was processed via the Illumina Novaseq/MGI-2000 platform. The procedure yielded high-quality clean reads of 110.44 Gb of raw data (Table 1). All subsequent analyses were then applied to these clean reads. The clean Hi-C paired-end reads were initially mapped to the primary assembly using Bowtie2 v2.3.2¹⁴. Then, HiC-Pro v2.8.1¹⁵

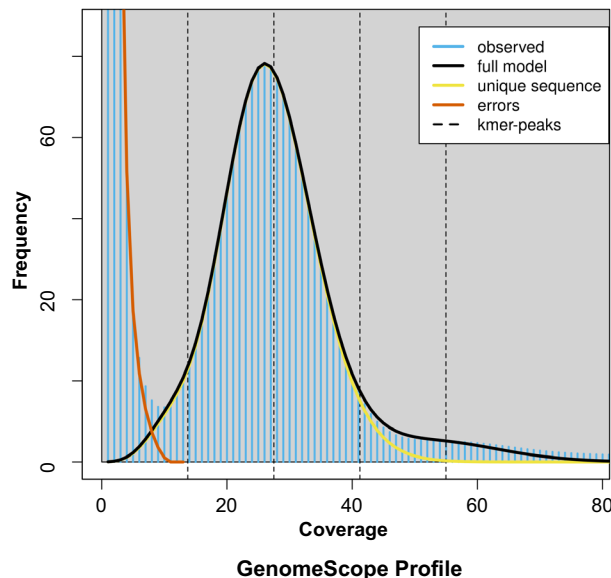


Fig. 1 The K-mer distribution of the *D. aiolomorphi* genome. len, genome haploid length; uniq, genome unique length; het, heterozygosity; kcov, genome coverage; err, read error rate; dup, duplicated sequence.

was utilized to identify valid alignments, simultaneously filtering out multiple hits and singletons alignments. Finally, Lachesis¹⁶ was employed to cluster, order and orient the scaffolds. Following Lachesis analysis, 1,083.41 Mb of reads were allocated to five pseudochromosomes, amounting to 99.89% of the final assembly (Fig. 2, Table 2).

Assessment of the genome assembly. To assess the completeness and accuracy of the final assembly of *D. aiolomorphi* genome, Benchmarking Universal Single Copy Orthologs (BUSCO) v5.2.2¹⁷ with the insect_obd10 database and hymenoptera_obd10 database were utilized. The assessments yielded high BUSCO scores of 97.3% and 91.1%, respectively (Fig. 3, Supplementary Table S2-3). Additionally, to ascertain the integrity of the genome assembly, the five pseudochromosomes from the final assembly were aligned to the Nt library to evaluate the genome assembly using BLAST v2.5.0¹⁸. Among the 5 chromosomes, 60% (3 pseudochromosomes) showed similarity to *Nasonia vitripennis*, 20% (1 pseudochromosomes) to *Eretmocerus* sp. and 20% (1 pseudochromosomes) to *Torymus* sp. These results suggest the pseudochromosomes sequences are free from sequences of non-target organisms, contaminants, or symbionts presented in the DNA library (Supplementary Table S4).

Repetitive element annotation. In the *D. aiolomorphi* genome, transposon element (TE) were identified using the Extensive *de novo* TE Annotator (EDTA) v1.9.6¹⁹. Tandem Repeats Finder (TRF) v4.09²⁰ facilitated the identification of tandem repeats. Based on these findings, a *de novo* repeat database was consequently generated using RepeatModeler v2.0.2²¹. The known repeats in Dfam database²² were combined with the results of TE detection and the *de novo* repeat database, creating a reference library that was clustered using Cd-hit v4.8.1²³ to eliminate redundant sequences. After combining and clustering, comprehensive repeat and TE detection was conducted using RepeatMasker v4.1.2 (<https://www.repeatmasker.org/>). The genome was found to have a total of 762.12 Mb repetitive sequences, accounting for 70.27% of the genome. Long Terminal Repeat (LTR) elements and DNA transposons emerged as the most predominant types of repeats, representing 24.40% and 22.60% of the genome, respectively (Table 3).

Protein-coding genes annotation. Transcriptome sequencing, homologous gene search and *de novo* prediction were employed to infer the protein-coding genes (PCGs) in the *D. aiolomorphi* genome, which were then integrated to generate a final gene set. Initially, transcriptome reads were aligned using Hisat2 v2.2.1²⁴ and assembled with StringTie v2.1.7²⁵. Meanwhile, Trinity v2.8.5²⁶ was utilized for *de novo* assembly of transcriptome reads. Subsequent mapping of the transcriptome assembly to the genome for gene structural prediction by PASA v2.3.3²⁷. For the identification of homologous gene sets, sequences from various insects, manually annotated in the Universal Protein Resource database (UniProt, <https://www.uniprot.org/>) and National Center for Biotechnology Information (NCBI, <https://www.ncbi.nlm.nih.gov/>), were aligned to the *D. aiolomorphi* genome using Exonerate v2.4.0²⁸ and Gemoma v1.7.1²⁹. The process of *de novo* gene prediction involved three separate programs, Augustus v3.3.3³⁰, SNAP v2.54.3³¹ and GeneMark-ETP v4.65³². A non-redundant consensus of gene structures was then generated by combining all results using EVIDENCEModeler v1.1.1³³. To annotate gene functions, the identified PCGs were aligned to various databases, including Nt, Nr, Swiss-Prot and TrEMBL, employing Diamond v2.0.5³⁴ with an e-value threshold of 1e-5. Protein classification and domain search were performed using eggNOG-mapper v2.1.4³⁵ and InterProScan v5.8.0³⁶. Finally, a total of 18,011 protein-coding genes were predicted, with 17,829 genes (98.99%) functionally annotated (Table 4).

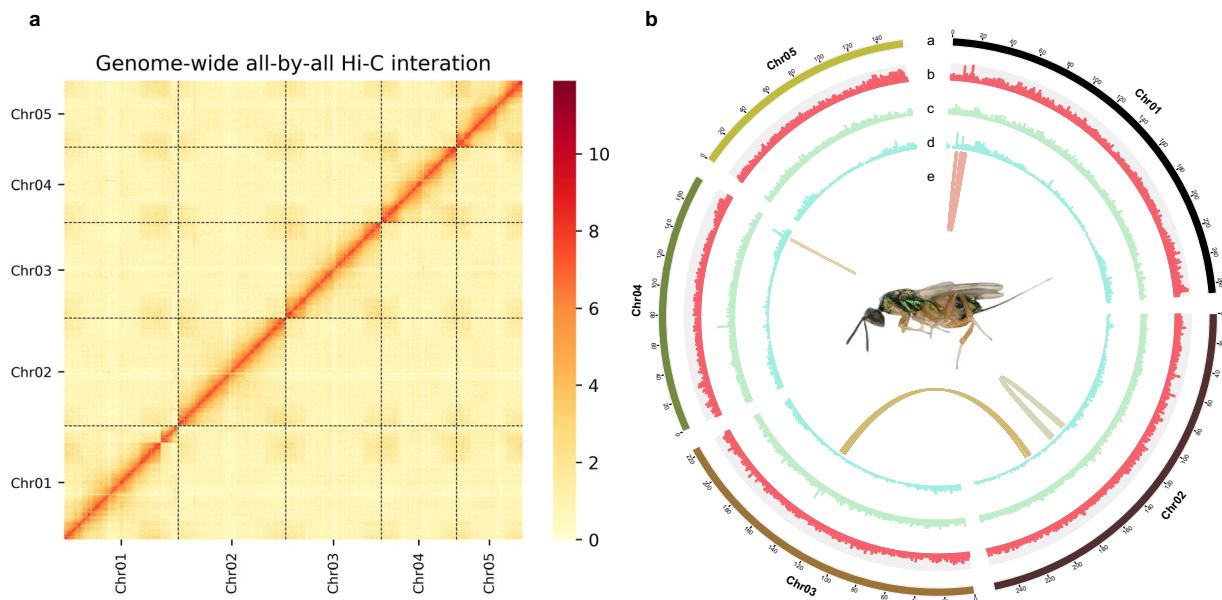


Fig. 2 Overview of the genomic features of the *D. aiolomorphi* genome. (a) Genome-wide all-by-all Hi-C interaction identified five pseudo-chromosome link groups of the *Diomorua aiolomorphi* genome; (b) Genomic features of the *D. aiolomorphi* genome. Tracks from outside to inside (a-e) are as follows: pseudo-chromosomes, GC contents, repeat density, gene density and collinearity between the pseudo-chromosomes.

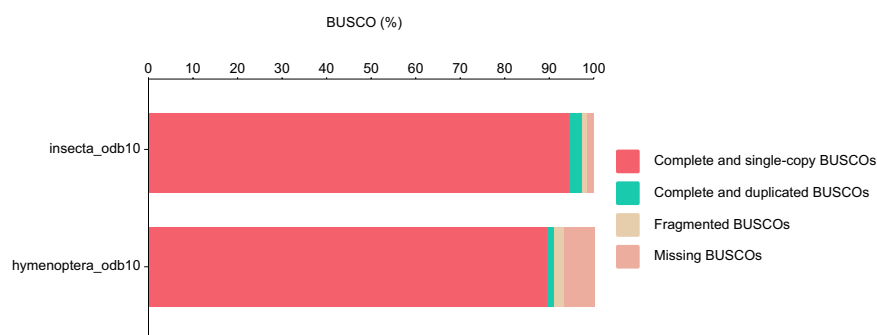


Fig. 3 The BUSCO summary of the *D. aiolomorphi* genome. The x axis represents the percentage of BUSCOs and the y axis represents BUSCO datasets.

Statistics	Number
Total length	1,084,575,061 bp
GC contents (%)	36.55%
The number of pseudo-chromosomes	5
Un scaffolded sequences	16
Contig N50	18,128,534 bp
Scaffold N50	224,866,539 bp
Total length of scaffold anchored to pseudo-chromosomes	1,083,519,070 bp
Total length of un scaffolded sequences	1,055,991 bp
Maximum length of un scaffolded sequence	143,167 bp
Maximum length of pseudo-chromosomes	267,152,207 bp
Minimum length of pseudo-chromosomes	157,366,800 bp

Table 2. Statistics of final Hi-C scaffolding genome of *D. aiolomorphi*.

Non-coding RNA annotation. To identify noncoding RNA, Basic Rapid Ribosomal RNA Predictor (BARRNAP) v0.9 and tRNAScan-SE v2.0.5³⁷ were executed for predicting rRNA and tRNA, respectively.

Items	Number of elements	Length occupied (bp)	Percentage of sequence (%)
SINEs	4,462	1,073,728	0.10
LINEs	68,416	43,695,187	4.03
LTR elements	537,852	264,598,312	24.40
DNA transposons	887,160	245,087,834	22.60
Unclassified	628,934	199,104,989	18.36
Satellites	1,590	428969	0.04
Simple repeats	324	10222	0.00

Table 3. Repeat elements statistics in the *D. aiolomorphi* genome. SINEs, short interspersed nuclear elements; LINEs, long interspersed nuclear elements; LTR, long terminal repeat.

Type	Number	Percent (%)
Total	18,011	—
Nr	10,905	60.55
Nt	6,488	36.02
Swiss-Prot	17,716	98.36
TrEMBL	10,622	58.98
EggNOG	10,538	58.51
InterProScan	7,043	39.10
Annotated	17,829	98.99
Unannotated	182	1.01

Table 4. Summary of the functional gene annotation of the *D. aiolomorphi* genome.

Infernal v1.1.2³⁸ was used to identify the remaining noncoding RNA based on the alignment with the Rfam library³⁹. Finally, 539 noncoding RNAs (ncRNAs) were predicted, including 57 micro-RNAs (miRNAs), 104 ribosomal RNAs (rRNAs), 21 small nuclear RNAs (snRNAs), 15 small nucleolar RNAs (snoRNAs), and 344 transfer RNAs (tRNAs) (Supplementary Table S5).

Data Records

The MGI, ONT, RNA-seq and Hi-C sequencing data used for the genome assembly were deposited in the NCBI Sequence Read Archive (SRA) database with accession numbers SRR26882530⁴⁰, SRR26882529⁴¹, SRR26882531⁴² and SRR26882528⁴³, respectively, under the BioProject accession number PRJNA1036143. The chromosome assembly was deposited at GenBank with accession number JAXKQO000000000⁴⁴. Genome annotation information was deposited in the Figshare database⁴⁵.

Technical Validation

To ensure the reliability and integrity of the genomic data, we implemented rigorous preprocessing protocols on various datasets (Illumina sequencing system protocol: https://support.illumina.com/content/dam/illumina-support/documents/documentation/system_documentation/novaseq/1000000019358_17_novaseq-6000-system-guide.pdf; Nanopore sequencing system protocol: https://a.storyblok.com/f/196663/x/a2ee9a9945/j2586-promethion-24-combined-qsg_170x250mm_rev2-final.pdf), including Illumina paired-end sequenced DNA raw short-reads, Nanopore sequenced DNA raw long-reads, Illumina paired-end sequenced RNA raw reads and Illumina paired-end Hi-C sequences. This preprocessing was carried out using fastp v.0.21.6⁴⁶, a widely recognized tool in genomic studies. The primary objective of this preprocessing step was to filter out low-quality sequences (Quality scores < 20), adapter sequences, reads containing Poly-N and sequences shorter than 30 bp. Following these stringent filtering criteria, we successfully obtained clean reads, which were subsequently stored in the fastq/fastq format.

Code availability

If no detailed parameters were mentioned, all software and tools in this study were performed according to those manuals and protocols of the applied bioinformatics software. No specific code or script was used in the study.

Received: 5 March 2024; Accepted: 15 August 2024;

Published online: 29 August 2024

References

- Shibata, E. Spatial density-independent parasitism of the inquiline, *Diomorus aiolomorphi* (Hymenoptera: Torymidae), on the bamboo gall maker, *Aiolomorphus rhopaloides* (Hymenoptera: Eurytomidae). *Appl. Entomol. Zool.* **41**, 493–498 (2006).
- Shibata, E. Sampling procedure for density estimation of bamboo galls induced by *Aiolomorphus rhopaloides* (Hymenoptera: Eurytomidae) in a bamboo stand. *J. For. Res.* **8**, 0123–0126 (2003).
- Shibata, E. Oviposition site preference of the bamboo gall maker, *Aiolomorphus rhopaloides* (Hymenoptera: Eurytomidae), on bamboo in terms of plant-vigor hypothesis. *Appl. Entomol. Zool.* **40**, 631–636 (2005).

4. Takahashi, F. & Mizuta, K. Life cycles of a eurytomid wasp, *Aiolomorphous rhopaloides*, and three species of wasps parasitic on it. *Japanese J. Appl. Entomol. Zool.* **15**, 36–43 (1971).
5. Askew, R. R. On the biology of the inhabitants of oak galls of Cynipidae (Hymenoptera) in Britain. *Trans. Soc. Br. Entomol.* **14**, 237–268 (1961).
6. Sanver, D. & Hawkins, B. A. Galls as habitats: the inquiline communities of insect galls. *Basic Appl. Ecol.* **1**, 3–11 (2000).
7. Kamijio, K. A new species of the genus *Diomorus* Walker (Hymenoptera: Torymidae). *Insecta Matsumurana.* **27**, 16–17 (1964).
8. Marçais, G. & Kingsford, C. A fast, lock-free approach for efficient parallel counting of occurrences of *k*-mers. *Bioinformatics.* **27**, 764–770 (2011).
9. Vurture, G. W. *et al.* GenomeScope: fast reference-free genome profiling from short reads. *Bioinformatics.* **33**, 2202–2204 (2017).
10. Hu, J. *et al.* NextDenovo: an efficient error correction and accurate assembly tool for noisy long reads. *Genome Biol.* **25**, 107 (2024).
11. Koren, S. *et al.* Canu: scalable and accurate long-read assembly via adaptive *k*-mer weighting and repeat separation. *Genome Res.* **27**, 722–736 (2017).
12. Hu, J., Fan, J. P., Sun, Z. Y. & Liu, S. L. NextPolish: a fast and efficient genome polishing tool for long-read assembly. *Bioinformatics.* **36**, 2253–2255 (2020).
13. Lieberman-Aiden, E. *et al.* Comprehensive mapping of long-range interactions reveals folding principles of the human genome. *Science.* **326**, 289–293 (2009).
14. Langmead, B. & Salzberg, S. L. Fast gapped-read alignment with Bowtie 2. *Nat. Methods* **9**, 357–359 (2012).
15. Servant, N. *et al.* HiC-Pro: an optimized and flexible pipeline for Hi-C data processing. *Genome Biol.* **16**, 259 (2015).
16. Burton, J. N. *et al.* Chromosome-scale scaffolding of *de novo* genome assemblies based on chromatin interactions. *Nat. Biotechnol.* **31**, 1119–1125 (2013).
17. Simao, F. A., Waterhouse, R. M., Ioannidis, P., Kriventseva, E. V. & Zdobnov, E. M. BUSCO: assessing genome assembly and annotation completeness with single-copy orthologs. *Bioinformatics.* **31**, 3210–3212 (2015).
18. Altschul, S. F., Gish, W., Miller, W., Myers, E. W. & Lipman, D. J. Basic local alignment search tool. *J. Mol. Biol.* **215**, 403–410 (1990).
19. Ou, S. J. *et al.* Benchmarking transposable element annotation methods for creation of a streamlined, comprehensive pipeline. *Genome Biol.* **20**, 275 (2019).
20. Benson, G. Tandem repeats finder: a program to analyze DNA sequences. *Nucleic Acids Res.* **27**, 573–580 (1999).
21. Flynn, J. M. *et al.* RepeatModeler2 for automated genomic discovery of transposable element families. *Proc. Natl. Acad. Sci. USA* **117**, 9451–9457 (2020).
22. Storer, J., Hubley, R., Rosen, J., Wheeler, T. J. & Smit, A. F. The Dfam community resource of transposable element families, sequence models, and genome annotations. *Mob. DNA* **12**, 2 (2021).
23. Li, W. Z. & Godzik, A. Cd-hit: a fast program for clustering and comparing large sets of protein or nucleotide sequences. *Bioinformatics.* **22**, 1658–1659 (2006).
24. Kim, D., Paggi, J. M., Park, C., Bennett, C. & Salzberg, S. L. Graph-based genome alignment and genotyping with HISAT2 and HISAT-genotype. *Nat. Biotechnol.* **37**, 907–915 (2019).
25. Pertea, M. *et al.* StringTie enables improved reconstruction of a transcriptome from RNA-seq reads. *Nat. Biotechnol.* **33**, 290–295 (2015).
26. Haas, B. J. *et al.* *De novo* transcript sequence reconstruction from RNA-seq using the Trinity platform for reference generation and analysis. *Nat. Protoc.* **8**, 1494–1512 (2013).
27. Haas, B. J. *et al.* Improving the *Arabidopsis* genome annotation using maximal transcript alignment assemblies. *Nucleic Acids Res.* **31**, 5654–5666 (2003).
28. Slater, G. S. & Birney, E. Automated generation of heuristics for biological sequence comparison. *BMC Bioinform.* **6**, 31 (2005).
29. Keilwagen, J. *et al.* Using intron position conservation for homology-based gene prediction. *Nucleic Acids Res.* **44**, 9 (2016).
30. Stanke, M. & Waack, S. Gene prediction with a hidden Markov model and a new intron submodel. *Bioinformatics.* **19**, II215–II225 (2003).
31. Korf, I. Gene finding in novel genomes. *BMC Bioinform.* **5**, 59 (2004).
32. Bruna, T., Lomsadze, A. & Borodovsky, M. GeneMark-ETP: automatic gene finding in eukaryotic genomes in consistency with extrinsic data. *bioRxiv*. <https://doi.org/10.1101/2023.01.13.524024> (2023).
33. Haas, B. J. *et al.* Automated eukaryotic gene structure annotation using EVIDENCEModeler and the program to assemble spliced alignments. *Genome Biol.* **9**, R7 (2008).
34. Buchfink, B., Reuter, K. & Drost, H. G. Sensitive protein alignments at tree-of-life scale using DIAMOND. *Nat. Methods* **18**, 366–368 (2021).
35. Cantalapiedra, C. P., Hernández-Plaza, A., Letunic, I., Bork, P. & Huerta-Cepas, J. eggNOG-mapper v2: functional annotation, orthology assignments, and domain prediction at the metagenomic scale. *Mol. Biol. Evol.* **38**, 5825–5829 (2021).
36. Zdobnov, E. M. & Apweiler, R. InterProScan - an integration platform for the signature-recognition methods in InterPro. *Bioinformatics.* **17**, 9 (2001).
37. Chan, P. P., Lin, B. Y., Mak, A. J. & Lowe, T. M. tRNAscan-SE 2.0: improved detection and functional classification of transfer RNA genes. *Nucleic Acids Res.* **49**, 16 (2021).
38. Nawrocki, E. P. & Eddy, S. R. Infernal 1.1: 100-fold faster RNA homology searches. *Bioinformatics.* **29**, 2933–2935 (2013).
39. Nawrocki, E. P. *et al.* Rfam 12.0: updates to the RNA families database. *Nucleic Acids Res.* **43**, D130–D137 (2015).
40. NCBI Sequence Read Archive. <https://identifiers.org/ncbi/insdc.sra:SRR26882530> (2023).
41. NCBI Sequence Read Archive. <https://identifiers.org/ncbi/insdc.sra:SRR26882529> (2023).
42. NCBI Sequence Read Archive. <https://identifiers.org/ncbi/insdc.sra:SRR26882531> (2023).
43. NCBI Sequence Read Archive. <https://identifiers.org/ncbi/insdc.sra:SRR26882528> (2023).
44. NCBI GenBank. <https://identifiers.org/nucleotide:JAXKQO000000000> (2023).
45. Ruizhong, Y. *et al.* Protein-coding genes annotation of the *Diomorus aiolomorphi* genome. *figshare* <https://doi.org/10.6084/m9.figshare.24785745> (2023).
46. Chen, S. F., Zhou, Y. Q., Chen, Y. R. & Gu, J. Fastp: an ultra-fast all-in-one FASTQ preprocessor. *Bioinformatics.* **34**, 884–890 (2018).

Acknowledgements

This study was supported by the Key International Joint Research Program of National Natural Science Foundation of China (31920103005), the General Program of National Natural Science Foundation of China (32070467), the National Key Research and Development Program of China (2023YFD1400600), the Provincial Key Research and Development Plan of Zhejiang (2021C02045) and the Key Project of Laboratory of Lingnan Modern Agriculture (NT2021003).

Author contributions

Conceptualization and supervision: Pu Tang and Xuexin Chen; Software: Ruizhong Yuan, Qiuyu Qu, Shiji Tian, Yu Jin, Jiabao Gong & Xiqian Ye; Investigation: Ruizhong Yuan, Qiuyu Qu, Zhaohe Lu & Xiansheng Geng; Writing – Original Draft Preparation: Ruizhong Yuan & Qiuyu Qu; Writing – Review & Editing: Ruizhong Yuan, Qiuyu Qu, Pu Tang & Xuexin Chen; Visualization: Ruizhong Yuan & Qiuyu Qu; Funding Acquisition: Pu Tang & Xuexin Chen.

Competing interests

The authors declare that they have no known competing financial interests or personal relationships that could have appeared to influence the work reported in this paper.

Additional information

Supplementary information The online version contains supplementary material available at <https://doi.org/10.1038/s41597-024-03779-y>.

Correspondence and requests for materials should be addressed to P.T. or X.C.

Reprints and permissions information is available at www.nature.com/reprints.

Publisher's note Springer Nature remains neutral with regard to jurisdictional claims in published maps and institutional affiliations.



Open Access This article is licensed under a Creative Commons Attribution-NonCommercial-NoDerivatives 4.0 International License, which permits any non-commercial use, sharing, distribution and reproduction in any medium or format, as long as you give appropriate credit to the original author(s) and the source, provide a link to the Creative Commons licence, and indicate if you modified the licensed material. You do not have permission under this licence to share adapted material derived from this article or parts of it. The images or other third party material in this article are included in the article's Creative Commons licence, unless indicated otherwise in a credit line to the material. If material is not included in the article's Creative Commons licence and your intended use is not permitted by statutory regulation or exceeds the permitted use, you will need to obtain permission directly from the copyright holder. To view a copy of this licence, visit <http://creativecommons.org/licenses/by-nc-nd/4.0/>.

© The Author(s) 2024